LIMITS ON STANDING WAVE CAVITY PERFORMANCE DUE TO THERMAL EFFECTS*

S. Smith[†], G. Burt, Lancaster University, Lancaster, UK
Cockcroft Institute, Daresbury Lab, UK

Abstract

After an RF cavity has been designed, a thermal analysis is typically performed to assess the effects of RF heating on the operating frequency and field flatness. A multi-physics approach (coupled electromagnetic, thermal, and mechanical) is normally employed, sometimes combined with computational fluid dynamics (CFD) simulations to incorporate flowing water, which is used for cooling in normal conducting structures. Performing a CFD analysis can add significant time to the design process because of the long and complex simulations and instead, approximations of the heat transfer coefficients and inlet/outlet water temperature rises are made and used directly in the multi-physics analysis. In this work, we explore these approximations, through the use of coupled electromagnetic-thermal-structural simulations and a preliminary CFD analysis.

INTRODUCTION

Normal conducting RF cavities are typically cooled by passing water through copper pipes around the structure, with the temperature being changed to compensate for frequency shifts. These shifts are caused by the thermal expansion of the cavity which is in-turn caused by RF power dissipation in the cavity walls. An analysis of these heating effects in generally left until the end of a design, and approximations are normally made about the heat transfer coefficient between the water and the copper walls and the temperature rise of the water as it passes through the pipes [1]. A self consistent approach that takes all the physics of the heating problem into account can be used to identify when these approximations are valid and eventually can be used to investigate the ultimate power limits on normal conducting cavities.

ELECTROMAGNETIC DESIGN

The first step in the thermal analysis requires the RF losses to be calculate on the cavity walls. The cavity used for this study is a C-band (5.712 GHz) bi-periodic standing wave structure that has been designed for industrial use. The nominal average input power is 850 W and it produces a 2 MeV electron beam. The electromagnetic analysis was performed in Ansys HFSS with the RF surface losses being shown in Fig. 1 [2]. Once these losses have been calculated they are scaled to the average input power of the linac and exported for use in thermal simulations.
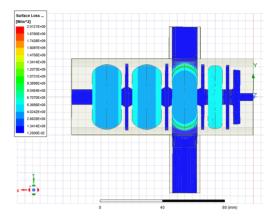
Figure 1: C-band linac showing RF surface losses.

BACKGROUND THEORY

The average temperature rise in the water used for cooling the structure can be estimated using [3]:

$$\Delta T = \frac{\dot{Q}}{c_p \cdot \dot{m}}, \tag{1}$$

where $\dot{Q}$ is the heat added to the system, c_p is the specific heat of the fluid and $\dot{m}$ is the mass flow rate of the fluid:

$$\dot{m} = \rho v A, \tag{2}$$

where v is the fluid velocity and A is the pipe cross sectional area. For an average input power of 850 W, and a mass flow rate of 0.08 kg/s a water temperature rise of 2.53 °C is obtained. The temperature difference between the water and the walls of the copper pipes is given by:

$$\Delta T = \frac{\dot{Q}}{hL\pi D}, \tag{3}$$

where L is the length of the pipe system, D is the hydraulic diameter and h is the heat transfer coefficient:

$$h = \frac{Nu \cdot \kappa}{D}, \tag{4}$$

where k is the thermal conductivity of the fluid and Nu is the Nusselt number given by:

$$Nu = \frac{(\frac{f}{8})(Re - 1000)Pr}{1 + 12.7(\frac{f}{8})^{1/2}(Pr^{2/3})}. \tag{5}$$

Re is the Reynold's number which provides information about whether the flow is turbulent or not. It is given by:

$$Re = \frac{\rho v D}{\eta} = \frac{994.1 \cdot 2.85 \cdot 0.06}{7.2 x 10^{-4}} = 23608 \tag{6}$$

where ρ is the density of water, v is the fluid velocity and η is the dynamic viscosity. For the case of 6 mm pipes, a 0.08 kg/s mass flow rate and water at 35 °C a Reynold's number of 23608 is obtained which is well over the threshold for turbulent flow (≈ 4000). The Prandtl number describes the ratio of viscous to thermal diffusion and is given by:

$$Pr = \frac{\eta \cdot c_p}{\kappa}. \tag{7}$$

Finally, f is the friction coefficient, which is given by:

$$f = [0.79 ln(Re) - 1.64]^{-2}. \tag{8}$$

The input parameters and calculated values are summarised in Table 1.

Table 1: Input Parameters and Estimated Temperature Rises.

Parameter	Value	Units
Pipe diameter	6	mm
Water density	994.1	kg/m^3
Initial mass flow rate	0.08	kg/s
Fluid velocity	2.85	m/s
Average input power	850	W
Dynamic viscosity	7.191×10^{-4}	Ns/m^2
Prandtl number	4.85	-
Reynolds number	23608	-
Friction coefficient	0.0251	-
Nusselt number	147.8	-
Heat transfer coefficient	14083.6	W/(m^{2}K)
Water temperature rise	2.53	°C
Boundary temperature rise	5.4	°C

COUPLED SIMULATIONS

A coupled electromagnetic-thermal-mechanical simulation was set up to provide an initial estimate of the temperature rise in the linac. For the steady-state (SS) thermal simulation, water pipes were placed around the linac as a single circuit and a constant temperature of 35 °C was applied to the water boundary. The losses from HFSS were imported, scaled to an input power or 850 W and applied to the faces of the structure that see the RF. The results are shown in Fig. 3, where a 7.25 °C temperature rise is seen between the iris and the fixed water and a ≈ 4.1°C rise between the hottest iris and the equator.

This temperature map was then imported into the static structural solver in order to investigate the deformation that this temperature increase would cause throughout the linac. Although in reality the linac would be secured in all directions causing strain in the copper, zero displacement boundaries were only set at either end of the linac in order to see the effects of the deformation.

EFFECTS ON FIELDS AND FREQUENCY

The resulting displacement was then re-imported into HFSS to look at the effects on the frequency and field flatness.
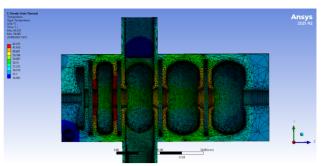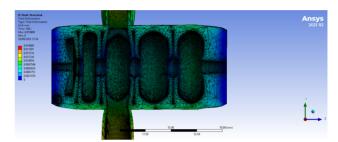
Figure 2: Steady state thermal simulation results.

Figure 3: Structural solver results showing up to 8 μm deformation on the cell walls.

The displaced mesh was simulated and a frequency shift of 1.5 MHz was found along with an induced error in the cavity fields which are shown in in Fig. 4.
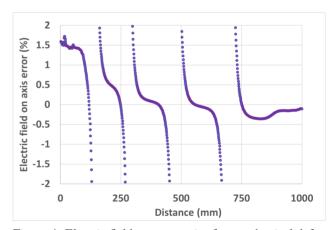

Figure 4: Electric field error on axis after mechanical deformation.

The largest errors are seen in the first second and last cells, as expected as these cells undergo the most deformation when the linac is fixed at either end. Large errors are also seen at the transition regions as the point where the electric field goes to zero shifts slightly as the cavity is deformed.

PRELIMINARY CFD SIMULATIONS

In order to get a more accurate estimate of the temperature rise in the water, a CFD simulation was set up in Ansys CFX. In this simulation the real water flow was included, with an applied heat flux on the cavity walls representing the RF surface losses. A pipe roughness of 20 μm was used and

convection to air was included with a heat transfer coefficient of 5 W/(m^{2}K) [4]. The temperature increase along the walls of the pipes is shown in Fig. 5, with an average temperature rise of 2.2 °C seen in the water from the inlet to the outlet.

Table 2: Comparison of Results.

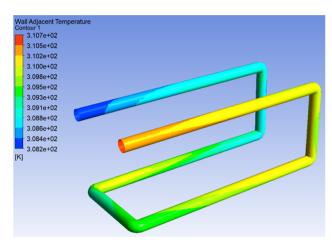| Quantity	Analytical	SS	CFD
Water ΔT	2.5 °C	0	2.2 °C
Boundary ΔT	5.4 °C	-	4.1 °C
Iris to equator ΔT	-	4.1 °C	4.7 °C

Figure 5: Ansys CFX results showing the wall adjacent temperature along the length of the cooling pipes.

The temperature rise inside the copper is shown in Fig. 6, with a maximum iris temperature of 49.05 °C, and a 4.6 °C rise between the hottest iris and the equator. Finally, the temperature rise across the pipe boundary layer is shown in Fig. 7. The analytical prediction of the water temperature rise agrees well with the CFD analysis, but there is a larger discrepancy between the boundary layer values. This is most likely due to the boundary layer not being fully resolved in the CFD analysis.

CONCLUSIONS AND FUTURE WORK

An initial thermal study study on a C-band electron linac has been performed as a starting point for the development of a full self-consistent thermal modelling approach. Analytical estimates of the water temperature rise have been made and compared with a CFD analysis with the same input parameters, giving good agreement. The effects of the cavity deformation have been investigated using a coupled simulation approach, with estimates of the frequency shift and introduced field errors given. In the future, improvements will be made when modelling the fluid boundary layer, and then this approach will be applied to a number of structures to investigate how these effects scale with frequency and cavity type.
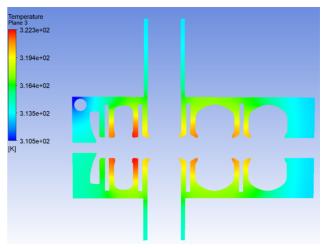

Figure 6: Ansys CFX results showing the temperature inside the structure.
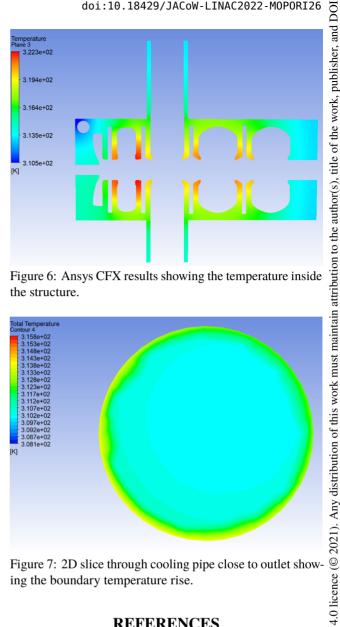

Figure 7: 2D slice through cooling pipe close to outlet showing the boundary temperature rise.

REFERENCES

[1] S. V. Kutsaev *et al.*, "Design and multiphysics analysis of a 176 mhz continuous-wave radio-frequency quadrupole," *Phys. Rev. ST Accel. Beams*, vol. 17, p. 072 001, 7 2014. doi:10.1103/PhysRevSTAB.17.072001

[2] Ansys®, *Academic Research Workbench, Release 21.2*, https://www.ansys.com/en-gb/products, Computer code, 2021.

[3] S. Pitman, "Optimisation studies for a high gradient proton linac for application in proton imaging: Probe: Proton boosting linac for imaging and therapy," English, Ph.D. dissertation, Lancaster University, 2019. doi:10.17635/lancaster/thesis/733

[4] K. Papke, C. Rossi, and G. C. Burt, "Coupled RF-Thermo-Structural Analysis of CLIC Traveling Wave Accelerating Structures," CERN, Tech. Rep., 2020. https://cds.cern.ch/record/2730555